Received 2009 December 1; accepted 2010 May 3
Preprint typeset using LaTeX style emulateapj v. 11/10/09

arXiv:1005.0470v1 [astro-ph.HE] 4 May 2010

GROWTH OF MASSIVE BLACK HOLES AT THEIR LATE STAGE

Ya-Di Xu[1], Xinwu Cao[2]
[1]Physics Department, Shanghai Jiao Tong University, 800 Dongchuan Road, Shanghai 200240, China and
[2]Key Laboratory for Research in Galaxies and Cosmology, Shanghai Astronomical Observatory, Chinese Academy of Sciences, 80 Nandan Road, Shanghai 200030, China
Email: ydxu@sjtu.edu.cn, cxw@shao.ac.cn

Received 2009 December 1; accepted 2010 May 3

ABSTRACT

It is believed that the local massive black holes were dominantly grown up through accretion during quasar phases, while a fraction of the local black hole mass was accumulated through accreting gases at very low rates. We derive the black hole mass density as a function of redshift with the bolometric luminosity function of active galactic nuclei (AGN) assuming that massive black holes grew via accreting the circumnuclear gases, in which the derived black hole mass density is required to match the measured local black hole mass density at $z = 0$. Advection dominated accretion flows (ADAFs) are supposed to present in low luminosity active galactic nuclei (AGNs)/normal galaxies, which are very hot and radiate mostly in the hard X-ray band. Most of the X-ray background (XRB) is contributed by bright AGNs, and a variety of AGN population synthesis models were developed to model the observed XRB in the last two decades. Based on our derived black hole mass density, we calculate the contribution to the XRB from the ADAFs in faint AGNs/normal galaxies with a given Eddington ratio distribution, which is mostly in hard X-ray energy band with an energy peak at ~ 200 keV. The growth of massive black holes during ADAF phase can therefore be constrained with the observed XRB. Combining an AGN population synthesis model with our results, we find that the fitting on the observed XRB, especially at hard X-ray energy band with $\gtrsim 100$ keV, is improved provided the contribution of the ADAFs in low-luminosity AGNs/normal galaxies is properly included. It is found that less than ∼15 per cent of local massive black hole mass density was accreted during ADAF phases. We suggest that more accurate measurements of the XRB in the energy band with $\gtrsim 100$ keV in the future may help constrain the growth of massive black holes at their late stage. We also calculate their contribution to the extragalactic γ-ray background (EGRB), and find that less than $\sim 1\%$ of the observed EGRB is contributed by the ADAFs in these faint sources.

Subject headings: galaxies: active—quasars: general—accretion, accretion disks—black hole physics; X-rays: diffuse background

1. INTRODUCTION

It is well believed that almost all galaxies contain massive black holes at their centers, and a tight correlation was revealed between central massive black hole mass and the velocity dispersion of the galaxy (Ferrarese & Merritt 2000; Gebhardt et al. 2000). The growth of massive black holes at the centers of galaxies may probably be linked to accretion processes (Soltan 1982). Yu & Tremaine (2002) estimated the black hole masses from the stellar velocity dispersions of galaxies measured by the Sloan Digital Sky Survey (SDSS) using the empirical relation between black hole mass and the velocity dispersion, and the local black hole mass density was derived. They further calculated the black hole mass density accreted during optical bright quasar phases using an optical quasar luminosity function (LF), and found that the accreted mass density is consistent with the local black hole mass density estimated from the velocity dispersions, if a radiative efficiency ~ 0.1 is adopted for quasars (also see Marconi et al. 2004; Shankar et al. 2004; Hopkins et al. 2007; Shankar et al. 2009). This implies that the growth of massive black holes through accretion during optically bright quasar phases may probably be important, if a radiative efficiency ~ 0.1 is adopted. If the massive black holes are spinning rapidly, their radiative efficiency can be higher than that they adopted, the black hole mass density accreted during quasar phases would be lower than the measured local black hole mass density (e.g., Cao 2007; Cao & Li 2008; Li et al. 2010). Thus, one cannot neglect the contribution from accretion at low rates to the growth of massive black holes, provided the duration of accretion at low rates is as long as Hubble timescale.

The cosmological X-ray background (XRB) is mostly contributed by AGNs (Hasinger 1998; Sreekumar et al. 1998), which can be used to constrain massive black hole accretion history (e.g., Elvis et al. 2002). In the most popular synthesis models of the XRB based on the unification schemes for AGNs, the cosmological XRB contributed by Compton-thin AGNs can account for $\sim$ 80% of the observed XRB (e.g., Ueda et al. 2003; Gilli et al. 2007). The residual XRB can be explained provided the same number of Compton-thick AGNs with $\log N_{\rm H} = 24 - 25$ as those with $\log N_{\rm H} = 23 - 24$ is included (Ueda et al. 2003). di Matteo & Fabian (1997) have alternatively proposed that the hard XRB above 10 keV may be dominated by the thermal bremsstrahlung emission from the advection dominated accretion flows (ADAFs) in low-luminosity AGNs. Due to the difficulties on detecting Compton-thick AGNs, the space number density of Compton-thick AGNs is still quite debated (e.g., Ueda et al. 2003; Treister & Urry 2005;

Gilli et al. 2007; Treister et al. 2009). Based on the surveys with *Swift* and *INTEGRAL* satellites, Treister et al. (2009) suggested that the space number density of Compton-thick AGNs may be significantly lower than those adopted in the previous AGN population synthesis models to explain the observed XRB. Due to the uncertainty of the number density of Compton-thick AGNs, the residual XRB could be attributed to both the Compton-thick AGNs and the ADAFs in faint AGNs and normal galaxies. Therefore, the observed XRB can be used to constrain massive black hole accretion history at their late stage when they are accreting at low rates (Cao 2005, 2007). Cao (2007) calculated the contribution to the XRB from the ADAFs in faint AGNs/normal galaxies, and compared it with the residual XRB. Their results showed that less than ∼5 per cent of local massive black hole mass density was accreted during ADAF phases, otherwise the XRB contributed from ADAFs will surpass the observed residual XRB even if no Compton-thick AGNs are included. For simplicity, they adopted an average mass accretion rate for faint AGNs/normal galaxies in calculating the contribution of ADAFs to the XRB. The radiative efficiency of standard thin accretion disks in bright AGNs does not vary with mass accretion rate. However, the faint AGNs/normal galaxies may probably contain ADAFs, of which the radiative efficiencies vary with mass accretion rate (Narayan & Yi 1995). The average radiative efficiency for a population of sources containing ADAFs accreting at different rates can be calculated by weighing over the distribution of mass accretion rate. The Eddington ratios of AGNs spread over several orders of magnitude (e.g., Ho 2002; Hopkins et al. 2006; Cao & Xu 2007). The Eddington ratio distribution for accreting massive black hole holes derived from observations exhibits nearly a power-law distribution with an exponential cutoff at high Eddington ratio (Merloni & Heinz 2008; Hopkins & Hernquist 2009; Kauffmann & Heckman 2009). In this paper, we will adopt the Eddington ratio distribution of AGNs derived by Hopkins & Hernquist (2009) to calculate the contribution of faint AGNs/normal galaxies to the XRB. Compared with the residual XRB, the constraints on the fraction of local black hole mass accreted in ADAF phases are derived. The cosmological parameters $\Omega_{\rm M}=0.3$, $\Omega_\Lambda=0.7$, and $H_0=70$ km s^{-1} Mpc^{-1} have been adopted in this work.

2. BLACK HOLE MASS FUNCTIONS

In this section, we derive the black hole mass densities as functions of redshift in a similar way as that done in Cao (2007). In this work, we use the bolometric quasar luminosity function (QLF) derived by Hopkins et al. (2007) to calculate the black hole mass densities. We summarize our calculations as follows (see Cao 2007, for the details).

Hopkins et al. (2007)'s QLF is calculated by using a large set of observed quasar luminosity functions in various wavebands, from the IR through optical, soft and hard X-rays (see Hopkins et al. 2007, for the details),

$$\frac{{\rm d}\Phi(L,z)}{{\rm d}\log L}=\frac{\phi_*}{(L/L_*)^{\gamma_1}+(L/L_*)^{\gamma_2}},\tag{1}$$

with normalization ϕ_*, break luminosity L_*, faint-end slope γ_1, and bright-end slope γ_2. The break luminosity L_* evolves with the redshift is given by

$$\log L_*=(\log L_*)_0+k_{L,1}\xi+k_{L,2}\xi^2+k_{L,3}\xi^3,\tag{2}$$

and the two slopes γ_1 and γ_2 evolves with redshift as

$$\gamma_1=(\gamma_1)_0\left(\frac{1+z}{1+z_{\rm ref}}\right)^{k_{\gamma_1}},\tag{3}$$

and

$$\gamma_2=\frac{2(\gamma_2)_0}{\left(\frac{1+z}{1+z_{\rm ref}}\right)^{k_{\gamma_2,1}}+\left(\frac{1+z}{1+z_{\rm ref}}\right)^{k_{\gamma_2,2}}}.\tag{4}$$

The parameter ξ is

$$\xi=\log\left(\frac{1+z}{1+z_{\rm ref}}\right),\tag{5}$$

and $z_{\rm ref}=2$ is fixed. The best-fit parameters we adopted in this work are as follows: $\log\phi_*({\rm Mpc}^{-3})=-4.825\pm0.060$, $[\log L_*(3.9\times10^{33}{\rm erg\ s}^{-1})]_0=13.036\pm0.043$, $k_{L,1}=0.632\pm0.077$, $k_{L,2}=-11.76\pm0.38$, $k_{L,3}=-14.25\pm0.80$, $(\gamma_1)_0=0.417\pm0.055$, $k_{\gamma_1}=-0.623\pm0.132$, $(\gamma_2)_0=2.174\pm0.055$, $k_{\gamma_2,1}=1.460\pm0.096$, and $k_{\gamma_2,2}=-0.793\pm0.057$ (Hopkins et al. 2007).

In this work, all the sources described by this QLF $\Phi(L,z)$ are referred as active galaxies, which are supposed to have mass accretion rates $\dot m\gtrsim\dot m_{\rm crit}=0.01$ [defined as $\dot m=0.1\dot Mc^2/L_{\rm Edd}$, and $L_{\rm Edd}=1.3\times10^{38}$ erg s$^{-1}(M_{\rm bh}/{\rm M}_\odot)$] and contain standard radiative efficient accretion disks. The cosmological evolution of black hole mass density caused by accretion during active galaxy phases is described by

$$\frac{{\rm d}\rho_{\rm bh}^{\rm A}(z)}{{\rm d}z}=\frac{{\rm d}t}{{\rm d}z}\frac{1}{{\rm M}_\odot}\int\frac{(1-\epsilon)L}{\epsilon c^2}\frac{{\rm d}\Phi(L,z)}{{\rm d}\log L}{\rm d}\log L,\tag{6}$$

where $\Phi(L,z)$ is the bolometric QLF given by Hopkins et al. (2007), $\rho_{\rm bh}^{\rm A}(z)$ (in units of ${\rm M}_\odot$ Mpc^{-3}) is the black hole mass density accreted during active galaxy phases from $z_{\rm max}$ to z, and ϵ is the average radiative efficiency for active galaxies.

For those inactive galaxies with $L<10^{41}$ ergs s^{-1}, their mass accretion rates are very low. The term "inactive galaxies" used in this work does not mean that they are really inactive. Compared with active galaxies, the massive black holes in inactive galaxies are still accreting, but at low rates with $\dot m\lesssim\dot m_{\rm crit}=0.01$, and radiatively inefficient ADAFs are suggested to be present in inactive galaxies (e.g., Narayan 2002). The black hole mass density $\rho_{\rm bh}^{\rm B}(z)$ accreted during inactive galaxy phases between z and $z_{\rm max}$ can be calculated by

$$\frac{{\rm d}\rho_{\rm bh}^{\rm B}(z)}{{\rm d}z}=\frac{\rho_{\rm bh}^{\rm inact}(z)\dot m_{\rm inact}^{\rm aver}L_{\odot,{\rm Edd}}(1-\epsilon^{\rm ADAF})}{0.1{\rm M}_\odot c^2}\frac{{\rm d}t}{{\rm d}z},\tag{7}$$

where $\dot m_{\rm inact}^{\rm aver}$ is the average dimensionless mass accretion rate for the inactive galaxies, $\rho_{\rm bh}^{\rm inact}(z)$ is the black hole mass density of inactive galaxies at redshift z, $\epsilon^{\rm ADAF}$ is the average radiative efficiency of the ADAFs in those inactive galaxies. The radiative efficiency $\epsilon^{\rm ADAF}$ is usually much lower than 0.01, so we approximately adopt $\epsilon^{\rm ADAF}\simeq0$ in our calculations on black hole mass densities.

Assuming that the growth of massive black hole is dominated by accretion, the total black hole mass density is given by

$$\rho_{\rm bh}(z) \simeq \rho_{\rm bh}^{\rm acc}(z)+\rho_{\rm bh}(z_{\rm max}) = \rho_{\rm bh}^{\rm A}(z)+\rho_{\rm bh}^{\rm B}(z)+\rho_{\rm bh}(z_{\rm max}), \tag{8}$$

where $\rho_{\rm bh}(z_{\rm max})$ is the total black hole mass density at $z_{\rm max}$. For active galaxies, the black hole mass density at redshift z can be calculated from the QLF by

$$\rho_{\rm bh}^{\rm act}(z) = \frac{1}{\lambda_{\rm act}^{\rm aver} L_{\rm Edd,\odot}} \int L \frac{{\rm d}\Phi(L,z)}{{\rm d}\log L}{\rm d}\log L \quad {\rm M_{\odot} Mpc^{-3}}, \tag{9}$$

where $\Phi(L,z)$ is the bolometric QLF given by Eq. (1), and $\lambda_{\rm act}^{\rm aver} = L_{\rm bol}/L_{\rm Edd}$ is the average Eddington ratio for active galaxies. In this work, we adopt $\lambda_{\rm act}^{\rm aver} = 0.25$ as that derived from a large bright AGN sample (Kollmeier et al. 2006). The black hole mass density for inactive galaxies $\rho_{\rm bh}^{\rm inact}(z)$ can be calculated with

$$\rho_{\rm bh}^{\rm inact}(z) = \rho_{\rm bh}(z) - \rho_{\rm bh}^{\rm act}(z) = \rho_{\rm bh}^{\rm A}(z)+\rho_{\rm bh}^{\rm B}(z)+\rho_{\rm bh}(z_{\rm max})-\rho_{\rm bh}^{\rm act}(z). \tag{10}$$

We assume $\rho_{\rm bh}^{\rm act}(z) = 0.5\rho_{\rm bh}(z_{\rm max})$ at $z = z_{\rm max}$, i.e., a half of all massive black holes are active at $z_{\rm max}$, as that used in Marconi et al. (2004), and the black hole mass density $\rho_{\rm bh}(z_{\rm max}) = 2\rho_{\rm bh}^{\rm act}(z_{\rm max})$ is obtained from Eq. (9). Thus, the black hole mass density as function of redshift z can finally be calculated by integrating Eqs. (6) and (7) from $z_{\rm max}$ to z with Eqs. (8)-(10), when the three parameters, $\lambda_{\rm act}^{\rm aver}$, $\dot{m}_{\rm inact}^{\rm aver}$ and ϵ are specified. We adopt $z_{\rm max} = 5$ in all calculations, and the value of ϵ is tuned to make the derived total black hole mass density $\rho_{\rm bh}(z)$ match the local black hole mass density $\rho_{\rm bh}^{\rm local}(z) = 4.0 \times 10^5 {\rm M_{\odot}~Mpc^{-3}}$ at $z = 0$ (e.g., Salucci et al. 1999; Marconi et al. 2004), when the value of $\dot{m}_{\rm inact}^{\rm aver}$ is specified. The black hole mass accreted during $z \geq 5$, $\rho_{\rm bh}(z=5)$, should be $\ll \rho_{\rm bh}(0)$, which implies that it will make little difference on our calculations even if a better QLF is available for $z_{\rm max} > 5$. Thus, we will not extrapolate the present QLF to higher redshifts.

3. EDDINGTON RATIO DISTRIBUTION FOR INACTIVE GALAXIES

The observed Eddington ratio distribution can be described by

$$f_{\lambda}(\lambda) = \frac{{\rm d}N}{N{\rm d}\log\lambda} = C_0 \left(\frac{\lambda}{\eta}\right)^{-\kappa} \exp\left(-\frac{\lambda}{\eta}\right), \tag{11}$$

where λ is the Eddington ratio, $\lambda \equiv L/L_{\rm Edd}$, and C_0 is the normalization (Hopkins & Hernquist 2009). They suggested that $\kappa \approx 0.3 - 0.8$, and $\eta = 0.2 - 0.4$. This Eddington ratio distribution is consistent with the self-regulated black hole growth model, in which feedback produces a self-regulating "decay" or "blowout" phase after the AGN reaches some peak luminosity and begins to expel gas and shut down accretion (Hopkins et al. 2005a,b; Hopkins & Hernquist 2009).

In this work, we assume the distribution of dimensionless mass accretion rate have a similar form as Eq. (11),

$$f_{\rm m}(\dot{m}) = \frac{{\rm d}N}{N{\rm d}\log\dot{m}} = C_1 \left(\frac{\dot{m}}{\eta}\right)^{-\kappa_{\rm m}} \exp\left(-\frac{\dot{m}}{\eta}\right) \simeq C_2 \dot{m}^{-\kappa_{\rm m}}, \tag{12}$$

for low-luminosity AGNs with $\dot{m} < \dot{m}_{\rm crit}$, where C_2 is the normalization. In all our calculations, we drop the exponential term in (12), which is a good approximation because $\dot{m} < \dot{m}_{\rm crit} << \eta$, and the accretion rate distribution (12) is always normalized by assuming all inactive black holes to be accreting with rates in the range of $\dot{m}_{\rm min} \leq \dot{m} \leq \dot{m}_{\rm max} = \dot{m}_{\rm crit}$. Thus, the accretion rate distribution can be described by one parameter $\kappa_{\rm m}$ with specified mass accretion rate range for inactive galaxies. The standard thin accretion disks are present in bright quasars, while they will transit to ADAFs provided the mass accretion rates are lower than the critical value $\dot{m}_{\rm crit}$ (e.g., Narayan, Mahadevan & Quataert 1998; Narayan 2002). The critical dimensionless mass accretion rate $\dot{m}_{\rm crit} \simeq 0.01$ is suggested either by observations or theoretical model calculations (see Narayan 2002, for a review and references therein). For inactive galaxies with $\dot{m} \lesssim \dot{m}_{\rm crit}$, their average mass accretion rate can be calculated with

$$\dot{m}_{\rm inact}^{\rm aver} = \int_{\dot{m}_{\rm min}}^{\dot{m}_{\rm crit}} \dot{m} f_{\rm m}(\dot{m}) {\rm d}\log\dot{m}, \tag{13}$$

where the minimum accretion rate, $\dot{m}_{\rm min} = 1.0 \times 10^{-5}$ is adopted in all our calculations. Thus, the value of parameter $\kappa_{\rm m}$ corresponds to an average mass accretion rate $\dot{m}_{\rm inact}^{\rm aver}$.

4. CONTRIBUTIONS OF INACTIVE GALAXIES TO THE COSMOLOGICAL BACKGROUND RADIATION

We employ the approach suggested by Manmoto (2000) to calculate the global structure of an ADAF surrounding a massive black hole in the general relativistic frame. All the radiation processes are included in the global structure calculations (see Manmoto 2000, for details and the references therein). The global structure of an ADAF surrounding a $10^8 {\rm M_{\odot}}$ black hole with spin parameter a can be calculated, if the model parameters, dimensionless mass accretion rate $\dot{m}$, magnetic field strength relative to gas pressure β, defined as $p_{\rm m} = B^2/8\pi = (1-\beta)p_{\rm tot}$ ($p_{\rm tot} = p_{\rm gas} + p_{\rm m}$), the fraction of the released gravitational energy directly heating the electrons δ, and the conventional viscosity parameter α, are specified. The constraints on the values of these parameters were discussed in Cao (2007). We adopt the same values as that work, i.e., $\alpha = 0.2$, and $\beta = 0.8$, with which no global solution is available for $\dot{m} \gtrsim 0.01$. This is consistent with the observations (e.g., Narayan 2002). The value of δ is still a controversial issue. In most of our calculations, we adopt a conventional value of $\delta = 0.1$ as that adopted Cao (2007). We also calculate the case with $\delta = 0.01$ for comparison.

The inner region of the ADAF is very hot, and the temperature of protons can be as high as $\sim 10^{12}$K. Thus, γ-ray emission may be produced through the pion production processes in the proton-proton (p-p) collisions and subsequently decay of neutral pions, which can be described by (Mahadevan et al. 1997)

$$p + p \rightarrow\ p + p + \pi^0,\ \pi^0 \rightarrow\ \gamma_1 + \gamma_2. \tag{14}$$

The production of gamma rays through p-p collisions has been studied in several works (Dermer 1986; Giovannelli et al. 1982a,b). Stecker (1971) showed that the gamma-ray spectrum produced in unit volume of the flow from π^0 decay can be calculated by

$$L_\nu = h^2\nu\, f_\gamma(E_\gamma) = 2h^2\nu \int_{E_{\pi_{\rm min}}}^{\infty} {\rm d}E_\pi \frac{f_\pi(E_\pi)}{\sqrt{E_\pi^2 - m_\pi^2}} \quad {\rm GeV\ s^{-1}\ Hz^{-1}\ cm^{-3}}, \tag{15}$$

where E_π is the pion energy in GeV, m_π is the mass of the pion in GeV c^{-2}, $f_\pi(E_\pi)$ is the π^0 spectrum, and $E_{\pi_{\rm min}}$ is the minimum pion energy required to produce a gamma-ray with energy E_γ, which is described by

$$E_{\pi_{\rm min}} = E_\gamma + \frac{m_\pi^2}{4E_\gamma}. \tag{16}$$

The gamma-ray spectrum of an ADAF mainly depends on the density and temperature distributions of the ions. The π^0 spectrum is given by (Dermer 1986),

$$\begin{aligned} f_\pi(E_\pi) = {} & \frac{c n_{\rm p}^2}{4m_\pi \theta_{\rm p} K_2^2(1/\theta_{\rm p})} \int_1^\infty {\rm d}\gamma_{\rm r} \frac{(\gamma_{\rm r}^2 - 1)}{[2(\gamma_{\rm r}+1)]^{1/2}} \\ & \times \int_1^{\zeta/m_\pi} {\rm d}\gamma^* (\beta^*\gamma^*)^{-1} \frac{{\rm d}\sigma^*(\gamma^*;\gamma_{\rm r})}{{\rm d}\gamma^*} \\ & \times \{\exp[-q\gamma\gamma^*(1-\beta\beta^*)] - \exp[-q\gamma\gamma^*(1+\beta\beta^*)]\} \\ & {\rm cm^{-3}\ s^{-1}\ GeV^{-1}}, \end{aligned} \tag{17}$$

where $n_{\rm p}$ is the number density of ions, $\theta_{\rm p} = kT_{\rm i}/m_{\rm p}c^2$ is the dimensionless ion temperature, $E_\pi = \gamma m_\pi$ is the pion energy in the observer's frame, and $K_2(x)$ is the modified Bessel function of order 2. The differential cross section for the production of a neutral pion with Lorentz factor γ^* in the center-of-momentum system (CM) of two colliding protons with relative Lorentz factor $\gamma_{\rm r}$ is denoted by ${\rm d}\sigma^*(\gamma^*;\gamma_{\rm r})/{\rm d}\gamma^*$, which is given in Stecker (1971). The quantities q and ζ are defined as $q = [2(\gamma+1)]^{1/2}/\theta_{\rm p}$ and $\zeta = (S - 4m_{\rm p}^2 + m_\pi^2)/2S^{1/2}$, where $S = 2m_{\rm p}^2(\gamma_{\rm r}+1)$ (see Stecker 1971, for the details). Thus, both the X-ray and γ-ray spectra of an ADAF can be calculated when the global structure of the ADAF is available.

We perform a set of spectral calculations for ADAFs surrounding black holes with different masses, and find that the dependence of ADAF spectrum on black hole mass is almost perfectly linear in X-ray/γ-ray bands for $M_{\rm bh} \gtrsim 10^6{\rm M}_\odot$, provided all other parameters are fixed. Therefore we simply use the spectrum $l_E(\dot m)$ of an ADAF around a typical massive black hole, $10^8{\rm M}_\odot$, accreting at the rate $\dot m$ as a template spectrum to calculate the contribution of inactive galaxies in unit of co-moving volume to the XRB by multiplying $\rho_{\rm bh}^{\rm inact}(z)/10^8{\rm M}_\odot$ with the accretion rate distribution (12) (see Eq. 19 in this section). We can calculate the average spectrum of a population of ADAFs accreting at rates with a distribution given by (12),

$$L_{\rm E}(E) = \int_{\dot m_{\rm min}}^{\dot m_{\rm crit}} f_{\rm m}(\dot m) l_E(\dot m) {\rm d}\log \dot m, \tag{18}$$

where $l_E(\dot m)$ is X-ray and γ-ray spectrum from an ADAF surrounding a $10^8{\rm M}_\odot$ black hole accreting with $\dot m$.

The contribution of the ADAFs in all inactive galaxies to the cosmological background radiation can be calculated by

$$f(E) = \frac{1}{10^8{\rm M}_\odot} \int_0^{z_{\rm max}} \frac{\rho_{\rm bh}^{\rm inact}(z)(1+z)L_{\rm E}[(1+z)E]}{4\pi\, d_{\rm L}^2} \frac{{\rm d}V}{{\rm d}z}{\rm d}z, \tag{19}$$

where $L_{\rm E}(E)$ is the template spectrum of ADAFs surrounding $10^8{\rm M}_\odot$ black holes averaged over accretion rate $\dot m$.

5. RESULTS

We plot average dimensionless mass accretion rate $\dot m_{\rm inact}^{\rm aver}$ as a function of power $\kappa_{\rm m}$ of the accretion rate distribution (see Eq. 12) for the inactive galaxies in Fig. 1. As discussed in §2, we can calculate both active and inactive black hole mass densities as functions of redshift simultaneously using the bolometric QLF based on the assumption that the growth of massive black holes is dominated by mass accretion. We plot the total black hole mass density $\rho_{\rm bh}(z)$, the black hole mass densities $\rho_{\rm bh}^{\rm inact}(z)$ for inactive galaxies and $\rho_{\rm bh}^{\rm act}(z)$ for active galaxies, as functions of redshift z in Fig. 2, for different values of $\kappa_{\rm m}$ (i.e., $\dot m_{\rm act}^{\rm aver}$), respectively. The ratios of black hole mass densities $\rho_{\rm bh}^{\rm B}(z)$ accumulated during ADAF phases between z and $z_{\rm max}$ to the local black hole mass density $\rho_{\rm bh}^{\rm local} = 4 \times 10^5 M_\odot{\rm Mpc}^{-3}$ are also plotted in Fig. 2.

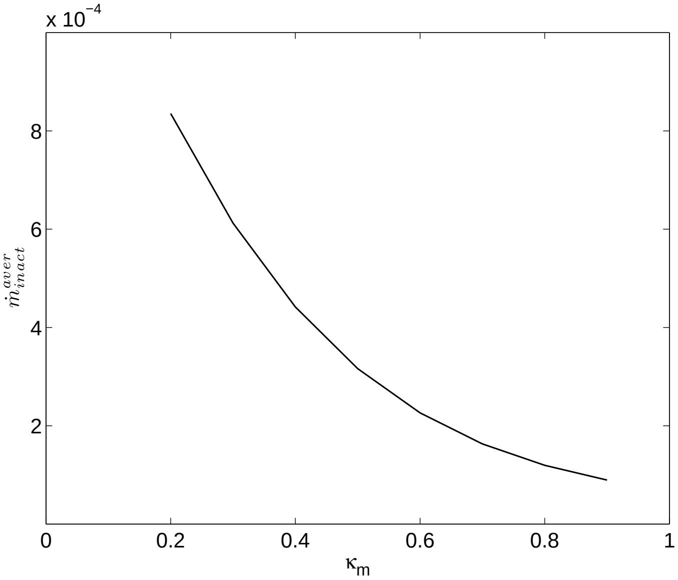

FIG. 1.— The relation of the power $\kappa_{\rm m}$ in Eq. (12) with average dimensionless mass accretion rate $\dot m_{\rm inact}^{\rm aver}$ for inactive galaxies. The minimum accretion rate, $\dot m_{\rm min} = 1.0 \times 10^{-5}$ is adopted in the calculations.The relation of the power $\kappa_{\rm m}$ in Eq. (12) with average dimensionless mass accretion rate $\dot m_{\rm inact}^{\rm aver}$ for inactive galaxies. The minimum accretion rate, $\dot m_{\rm min} = 1.0 \times 10^{-5}$ is adopted in the calculations.

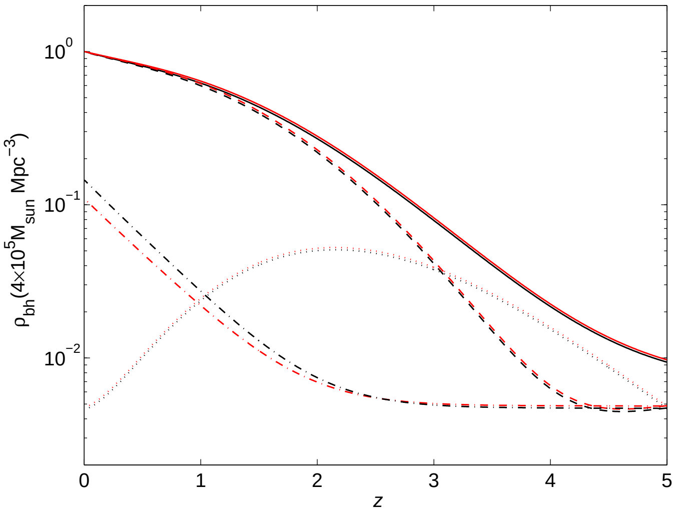

FIG. 2.— The total black hole mass densities $\rho_{\rm bh}(z)$ accumulated through accretion as functions of redshift z (solid lines) in unit of $\rho_{\rm bh}^{\rm local} = 4 \times 10^5 M_\odot {\rm Mpc}^{-3}$. The dashed and dotted lines represent the black hole mass densities $\rho_{\rm bh}^{\rm inact}(z)$ for inactive galaxies and $\rho_{\rm bh}^{\rm act}(z)$ for active galaxies at redshift z, respectively. The dot-dashed lines represent the ratio of black hole mass densities $\rho_{\rm bh}^{\rm B}(z)$ accumulated during ADAF phases to the local black hole mass density $\rho_{\rm bh}^{\rm local} = 4 \times 10^5 M_\odot {\rm Mpc}^{-3}$ from $z_{\rm max}$ to z. The different colors correspond to different values of $\kappa_{\rm m} = 0.2$ (black) and 0.3 (red).

The global structure of an ADAF surrounding a spinning massive black hole is available by solving a set of general relativistic hydrodynamical equations (see Manmoto 2000, for the details). The structures of ADAFs are plotted in Fig. 3 for different parameters, which show that the proton temperature in the inner edge of the ADAFs surrounding rapidly spinning black holes can be as high as $\sim 10^{12}$K. The spectra of ADAFs surrounding massive black holes can be calculated with the derived global structure of ADAFs (see §4). In Fig. 4, we plot the X-ray and γ-ray spectra of the ADAFs surrounding massive black holes with different values of spin parameter a. We also plot the spectra calculated with $\delta = 0.01$ in Fig. 5. In the calculations, the black hole mass $M_{\rm bh} = 10^8 {\rm M}_\odot$ is adopted. As the radiative efficiency of an ADAF is no longer constant, we calculate the bolometric luminosities of ADAFs as functions of mass accretion rate $\dot m$. Figure 6 shows how the Eddington ratios $L_{\rm bol}/L_{\rm Edd}$ vary with mass accretion rate $\dot m$ for different black hole spin parameters and ADAF parameters. The average X-ray and γ-ray spectra from a population of ADAFs, of which the mass accretion rate distribution is described by Eq. (12), are given in Fig. 7 for $\delta = 0.1$ and 0.01, respectively.

The average mass accretion rate $\dot m_{\rm inact}^{\rm aver}$ can be calculated with Eq. (13) for a specified index $\kappa_{\rm m}$ of the power law accretion rate distribution (12). For a given average mass accretion rate $\dot m_{\rm inact}^{\rm aver}$, the contribution of the ADAFs in all inactive galaxies to the X-ray/γ-ray background is calculated with the derived inactive black hole mass density and ADAF spectra. We plot the contribution of the ADAFs in all inactive galaxies to the X-ray band cosmological background with different black hole and ADAF parameters in Figs. 8 and 9. For comparison, we also plot the observed XRB in the figure, and the sum of the contributions from the type I/II bright AGNs(Compton-thin) given by Treister et al. (2009) and all inactive galaxies derived in this work. Their contribution to the extragalactic γ-ray background is plotted in Figs. 10 and 11 for $\delta = 0.1$ and 0.01, respectively.

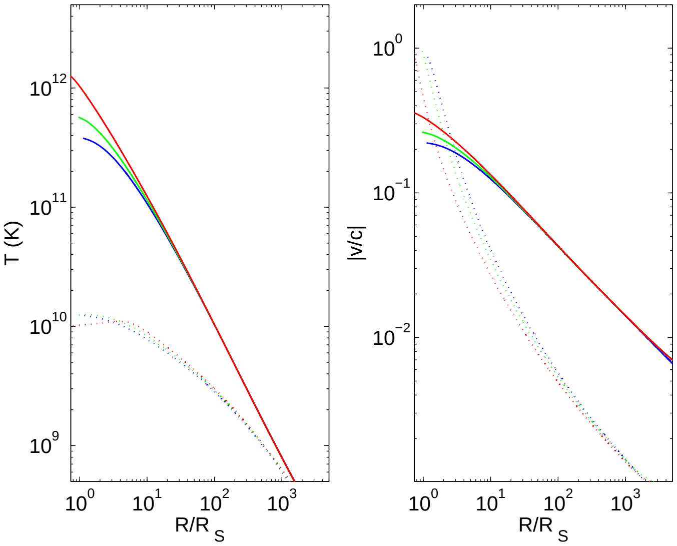

FIG. 3.— The structure profiles of the ADAFs surrounding a $10^8 M_\odot$ black hole with different spins, $a = 0.$ (blue lines), $a = 0.5$(green lines) and $a = 0.9$(red lines) accreting at $\dot m = 0.001$. Left panel: the temperature distributions of the electrons (dotted lines) and ions (solid lines) as functions of dimensionless radius $R/R_{\rm S}$ ($R_{\rm S} = 2GM/c^2$). Right panel: the radial velocity (dotted lines) and sound speed (solid lines) distributions. The parameter $\delta = 0.01$ is adopted in the calculations.

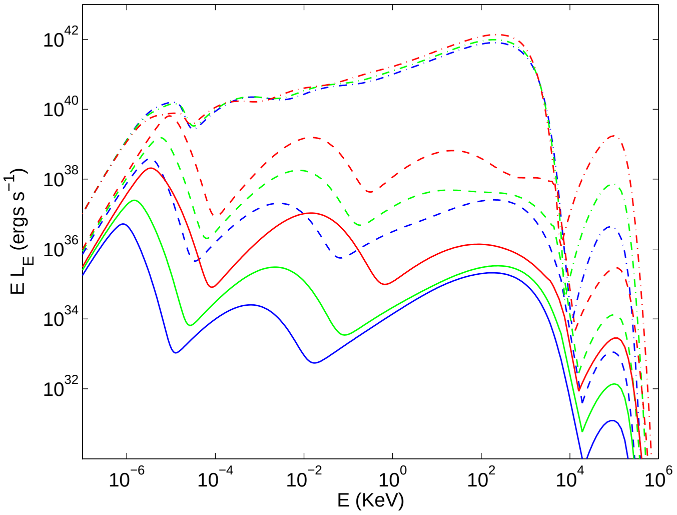

FIG. 4.— The X-ray/γ-ray spectra of the ADAFs surrounding a $10^8 M_\odot$ Schwarzschild (blue lines) or Kerr black hole with $a = 0.5$ (green lines) and $a = 0.9$ (red lines) accreting at different rates. The solid, dashed, and dash-dotted lines are corresponding to the accretion rates $\dot m = 1.0 \times 10^{-5}$, 1.0×10^{-4}, and 1.0×10^{-2}, respectively. The parameter $\delta = 0.1$ is adopted in the calculations.

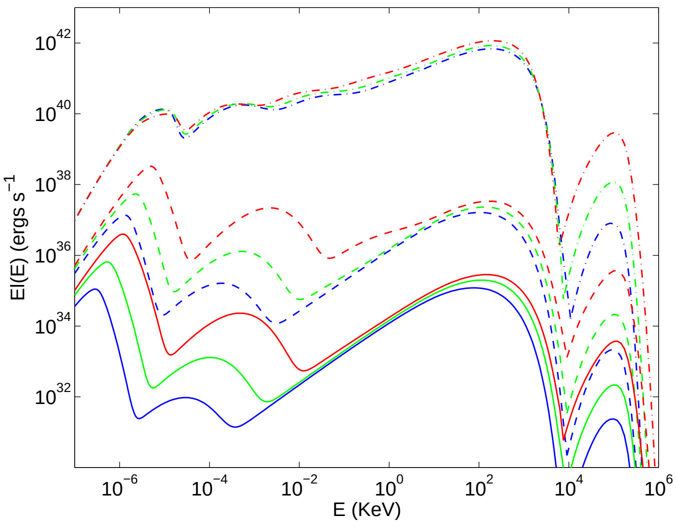

FIG. 5.— The same as Fig. 4, but the parameter $\delta = 0.01$ is adopted.

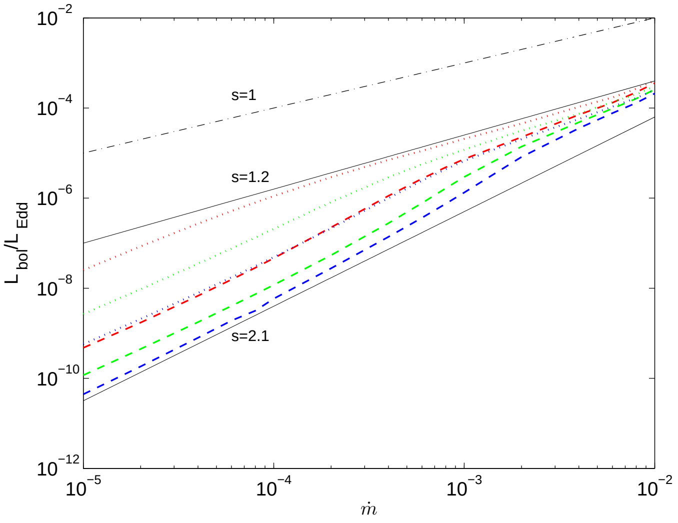

FIG. 6.— The relation between dimensionless mass accretion rate $\dot{m}$ and Eddington ratio $L_{\rm bol}/L_{\rm Edd}$ for ADAFs in inactive galaxies. The dotted and dashed lines represent the results for $\delta = 0.1$ and 0.01, respectively. The lines with different colors correspond to different values of $a = 0$ (blue), 0.5 (green), and 0.9 (red), respectively. For comparison, we also plot several power-law lines $L_{\rm bol}/L_{\rm Edd} \propto \dot{m}^s$ in the figure. The black dash-dotted line represents $s = 1$, i.e., constant radiative efficiency, and $\epsilon = 0.1$.

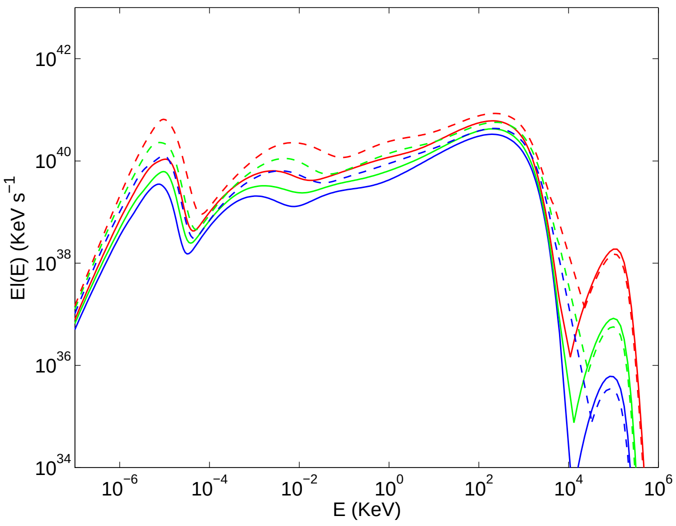

FIG. 7.— The X-ray and γ-ray spectra averaged over a population of ADAFs surrounding $10^8 M_\odot$ black holes, which has $\dot{m}$ distribution as indicated in Eq. 12, with different values of spin parameter a and ADAF model parameter δ. The different color lines represent the cases with spin parameter $a = 0$ (blue), 0.5 (green), and 0.9 (red), respectively. The solid and dashed lines correspond to the spectra with $\delta = 0.1$ and $\delta = 0.01$, respectively. The parameter $\kappa_{\rm m} = 0.3$ is adopted in the calculations.

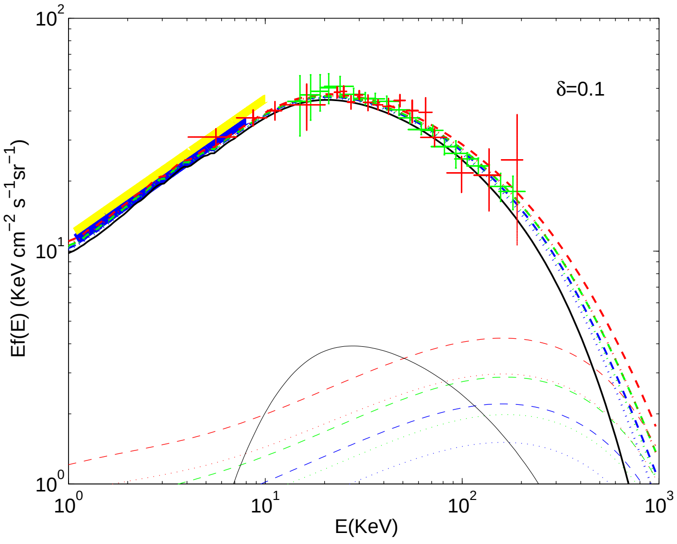

FIG. 8.— The contribution of the ADAFs in all inactive galaxies to the XRB. The thick black solid line represents the XRB spectrum from the AGN population synthesis model given by Treister et al. (2009). The thin solid line represents the contribution to their model from Compton-thick AGNs. The lower blue, green and red lines correspond to the contribution from all inactive galaxies with spin parameter $a = 0$, 0.5, and 0.9, respectively. The upper blue, green, and red lines correspond to the sum of X-ray contributions from both the AGN population synthesis model given by Treister et al. (2009) and all inactive galaxies. The dashed and dotted lines represent different values of $\kappa_{\rm m}$: 0.2 and 0.3, which correspond to average mass accretion rate of inactive galaxies $\dot{m}^{\rm aver}_{\rm inact} = 8.35 \times 10^{-4}$ and 6.12×10^{-4}, respectively. The parameter $\delta = 0.1$ is adopted in the calculations. The measurements of the extragalactic XRB with *Chandra* (Hickox & Markevitch 2006), *XMM* (De Luca & Molendi 2004), *INTEGRAL* (Churazov et al. 2007) and *Swift* (Ajello et al. 2008) are plotted as blue shaded area, yellow shaded area, red and green points, respectively.

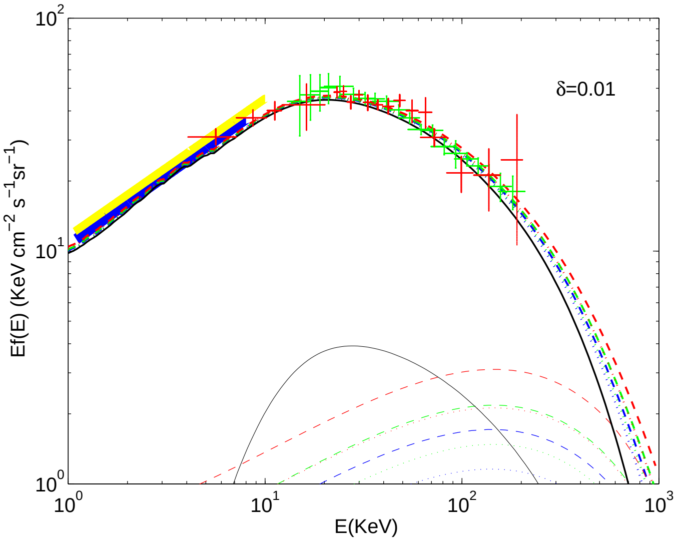

FIG. 9.— The same as Fig. 8, but the parameter $\delta = 0.01$ is adopted.

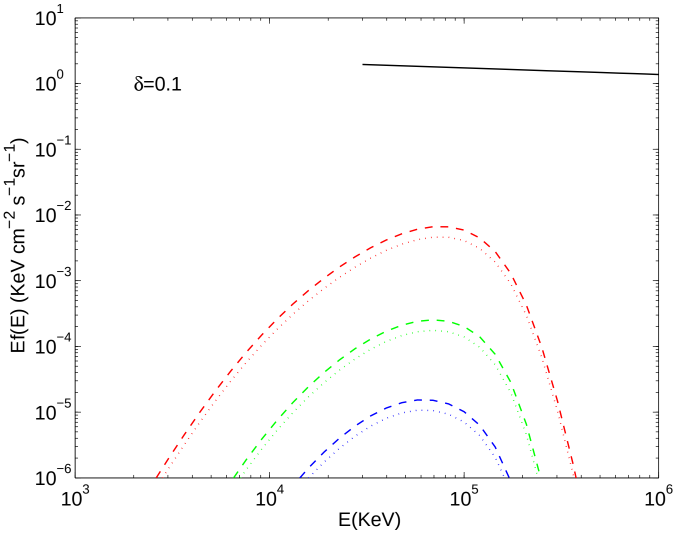

FIG. 10.— The contribution of the ADAFs in all inactive galaxies to the EGRB. The black solid line denotes the observed EGRB (taken from Sreekumar et al. 1998). The different color lines correspond to the contribution from ADAFs surrounding black holes in all inactive galaxies with spin parameter $a = 0$ (blue), 0.5 (green), and 0.9 (red), respectively.

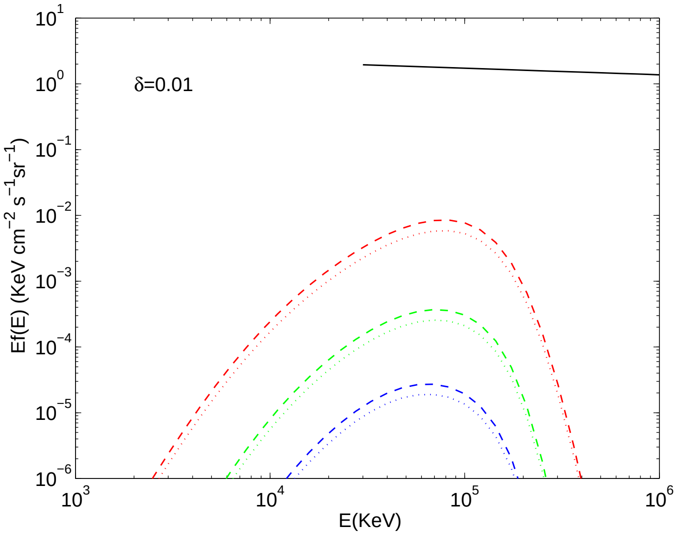

FIG. 11.— The same as Fig. 10, but the parameter $\delta = 0.01$ is adopted.

6. DISCUSSION

Unlike standard thin accretion disks, the radiative efficiency of ADAFs increases with mass accretion rate $\dot{m}$ (Narayan & Yi 1995). Thus, the average radiative efficiency for a population of ADAFs is available only if the distribution of mass accretion rate $\dot{m}$ is known. The Eddington ratio distribution for AGNs was extensively explored by different authors (e.g., Merloni & Heinz 2008; Hopkins & Hernquist 2009; Kauffmann & Heckman 2009). These works suggested that more sources are accreting at lower rates, and the Eddington ratios for AGNs can be well described by a power law distribution (Hopkins & Hernquist 2009). This implies that the average radiative efficiency for the ADAFs with this Eddington ratio distribution can be lower than that for an ADAF accreting at the average mass rate, because the radiative efficiency of ADAFs increases with mass accretion rate $\dot{m}$ (Narayan & Yi 1995). Cao (2007) calculated the contribution of ADAFs to the XRB, and the constraint on the fraction of black hole mass accreted in ADAF phases was derived by comparing with the residual XRB. An average mass accretion rate is adopted in Cao (2007)'s calculations for simplicity, and therefore the upper limit on the mass growth of black holes in ADAF phases is under-estimated. In this work, we improve the calculations by Cao (2007) by including the Eddington ratio distribution for AGNs in our calculations.

Using the method described in §2, the active, inactive and total black hole mass densities as functions of redshift are calculated by tuning the average radiative efficiency ϵ for active galaxies to let the total black mass density match the measured local black hole mass density at $z = 0$ (see Fig. 2). It is found that most of the local black hole mass was accumulated during $z \lesssim 2$, and fraction of the local black hole mass accreted during ADAF phases is determined by the average mass accretion rate $\dot{m}_{\rm inact}^{\rm aver}$, i.e., the distribution of accretion rates for inactive galaxies. We find that the average radiative efficiency $\simeq 0.134$ is required for active galaxies, which corresponds to $a \approx 0.9$. This is consistent with that derived in Cao (2007) and Elvis et al. (2002).

In the calculation of the black hole mass densities, we need to know the value of the average Eddington ratio for the active galaxies $\lambda_{\rm act}^{\rm aver}$, which is still uncertain. McLure & Dunlop (2004) estimated that the average accretion rate $\dot{m}_{\rm act}^{\rm aver}$ varies from 0.1 at $z \sim 0.2$ to 0.4 at $z \sim 2$ from a large sample of SDSS quasars. Kollmeier et al. (2006) estimated the black hole masses and Eddington ratios for a sample of luminous AGNs with $0.3 < z < 4$, and found that their average Eddington ratio is $\simeq 0.25$. We adopt $\lambda_{\rm act}^{\rm aver} = 0.25$ in this work in the calculation of active black hole mass density $\rho_{\rm bh}^{\rm act}(z)$ and then the inactive black hole mass density $\rho_{\rm bh}^{\rm inact}(z)$. The derived active black hole mass density $\rho_{\rm bh}^{\rm act}(z)$ is proportional to $1/\lambda_{\rm act}^{\rm aver}$ (see Eq. 9). We find that the derived $\rho_{\rm bh}^{\rm act}(z) \ll \rho_{\rm bh}^{\rm inact}(z)$ for $z \lesssim 3$ (see Fig. 2). The inactive black hole mass density $\rho_{\rm bh}^{\rm inact}(z)$ is calculated by subtracting the active black hole mass density $\rho_{\rm bh}^{\rm act}(z)$ from the total black hole mass density $\rho_{\rm bh}(z)$ at redshift z (see Eq. 10), and $\rho_{\rm bh}(z)$ is derived with QLF as required to match the measured local black hole mass density $\rho_{\rm bh}^{\rm local}$ at $z = 0$, which implies that the derived $\rho_{\rm bh}^{\rm inact}(z)$ is almost insensitive to the value of $\lambda_{\rm act}^{\rm aver}$ for $z \lesssim 3$. The XRB and growth of massive black holes are mainly contributed by the accretion in the sources at low redshifts, which implies that our main conclusions on the growth of massive black holes at their late stage will not be affected if the value of $\lambda_{\rm act}^{\rm aver}$ does not deviate much from the value adopted in this work. For the average radiative efficiency $\epsilon = 0.134$ derived in this work, the average mass accretion rate for active galaxies $\dot{m}_{\rm act}^{\rm aver} = 0.187$ corresponding to $\lambda_{\rm act}^{\rm aver} = 0.25$. The black hole mass densities can be calculated alternatively by using the Eddington ratio distribution given by Eq. 12. This distribution shows that most active galaxies have mass accretion rates $\dot{m}$ close to the critical one $\dot{m}_{\rm crit} = 0.01$ with an average $\dot{m}_{\rm act}^{\rm aver} \sim 0.1$ for $\kappa_{\rm m} = 0.3$. As discussed above, our main conclusions will not be altered either with this value or a distribution instead of a single average one. The contribution of all bright AGNs to the XRB can be directly calculated with the QLF, which is independent of the Eddington ratio distribution. Hopkins et al. (2007)'s calculation showed that the observed XRB can be roughly reproduced with their QLF.

Our calculations of the XRB contributed by ADAFs in inactive galaxies are sensitive to the spectra of ADAFs, which are described by several parameters, i.e., magnetic field strength relative to gas pressure β, the fraction of energy directly heating the electrons δ, and the viscosity parameter α. In Cao (2007)'s work, the theoretical/observational constraints on the values of these parameters were discussed, which leads to narrow ranges for the values of these parameters. The X-ray/γ-ray spectra of ADAFs are almost independent of the value of β (magnetic field strength), which only affects the spectra in radio bands. As we are focusing on the hard X-ray and γ-ray energy bands, we find that the spectra of ADAFs depend most sensitively on the value of δ, because the electron temperature in the ADAF is sensitively affected by the energy directly heating the electrons. Besides a conventional value of $\delta = 0.1$ adopted in our calculations, we also carry out the calculations with $\delta = 0.01$ for comparison. In this case, the radiative efficiency of ADAFs is lower than that for $\delta = 0.1$, as the heating of electrons is significantly suppressed (see Figs. 4-6).

Figure 6 shows how the Eddington ratios $L_{\rm bol}/L_{\rm Edd}$ vary with mass accretion rate $\dot{m}$ for different values of δ and black hole spin parameter a. We find that the Eddington ratio varies with $\dot{m}$ roughly as $L_{\rm bol}/L_{\rm Edd} \propto \dot{m}^s$, where $s \simeq 1.2 - 2.1$ depending on the values of parameters adopted. For comparison, we plot several power-law lines $L_{\rm bol}/L_{\rm Edd} \propto \dot{m}^s$, $s = 1$, i.e., constant radiative efficiency $\epsilon = 0.1$ (black dash-dotted line), $s = 1.2$ and 2.1 in the same figure. The result $s \simeq 1.2 - 2.1$ means that the radiative efficiencies of ADAFs increases with $\dot{m}$. Our results are consistent with those adopted in the previous works (Narayan & Yi 1995; Jester 2005; Hopkins et al. 2007). It is not surprising that the radiative efficiency increases with δ, and the bolometric luminosity $L_{\rm bol}$ is higher for rapidly spinning black holes provided the same accretion rate $\dot{m}$ is adopted.

Combining the derived inactive black hole mass density $\rho_{\rm bh}^{\rm inact}(z)$ and the average spectra of a population of ADAFs with the mass accretion rate distribution (Eq. 12), the contribution of the ADAFs in all inactive galaxies to the XRB can be calculated. The results are plotted in Figs. 8 and 9, which are compared with the observed XRB. The contribution of bright AGNs to the XRB was estimated in many previous works (e.g., Ueda et al. 2003; Treister & Urry 2005; Gilli et al. 2007; Treister et al. 2009). We compare the sum of the contribution of bright AGNs to XRB estimated by Treister et al. (2009) and that of the ADAFs in all inactive galaxies calculated in this work with the observed XRB. It is found that $\kappa_{\rm m} \gtrsim 0.3$ for $\delta = 0.1$ (or $\kappa_{\rm m} \gtrsim 0.2$ for $\delta = 0.01$) is required in order to let the calculated XRB not surpass the observed XRB (see Figs. 8 and 9). The dependence of required value of $\kappa_{\rm m}$ on parameter δ can be understood that, a smaller δ corresponds to a lower radiative efficiency, while a smaller $\kappa_{\rm m}$ represents a flatter dimensionless mass accretion rate distribution which has relatively more high- $\dot{m}(\approx 10^{-3} - 10^{-2})$ sources. The average mass accretion rate for inactive black holes is relatively high for a distribution with a small $\kappa_{\rm m}$, which also corresponds to a relatively high average radiative efficiency, because the radiative efficiency of an ADAF increases with $\dot{m}$ (see Fig. 6). This implies that the distribution with a too flat mass accretion distribution (i.e., small $\kappa_{\rm m}$) will over-produce sources accreting at rates close to $\dot{m}_{\rm max}$, which will radiates too much to the XRB. On the other hand, the value of κ_m can also be constrained by κ and s according to the relation $L_{\rm bol}/L_{\rm Edd} \propto \dot{m}^s$ and equations (11) and (12). Hopkins & Hernquist (2009) suggested $\kappa \approx 0.3 - 0.8$, and our calculation predicts $s \simeq 1.2 - 2.1$ for different parameters, then we can expect $\kappa_{\rm m} \approx \kappa s \approx 0.36 - 1.67$, which is roughly consistent with the constraints from comparison with the XRB in this work. Our results implies that the XRB contributed by inactive black holes is dominated by the radiation from high-$\dot{m}$ sources, rather than low-$\dot{m}$ sources.

The energy peak of the contribution of the ADAFs in inactive galaxies to the XRB is around $\sim 100 - 200$ keV depending on the values of δ, which accounts for $\sim 15 - 20\%$ of the XRB at these energy peaks (see Figs. 8 and 9). The *Swift* measurements on the XRB have estimated errors of $\sim 3\%$ (Ajello et al. 2008; Treister et al. 2009).

Thus, we suggest that more accurate measurements of the XRB in the energy band with $\gtrsim$ 100 keV in the future may constrain the growth of massive black holes at their late stage more precisely. We note that the peak energy of the contribution of Compton-thick AGNs is ~ 30 keV, while it is $\sim 100-200$ keV for that of ADAFs in inactive massive black holes. This implies that the constraints on the growth of massive black holes at their late stage from the XRB have hardly been affected by the possible uncertainty of the space number density of Compton-thick AGNs.

The values of $\kappa_{\rm m}$=0.2 and 0.3 correspond to average mass accretion rates of inactive galaxies $\dot{m}_{\rm inact}^{\rm aver} = 8.35 \times 10^{-4}$ and 6.12×10^{-4}, respectively (see Fig. 1). This means that the mass fraction of local black holes grown in ADAF phases should be less than 10.9% (for $\delta = 0.1$) and 14.5% (for $\delta = 0.01$) (see Fig. 2). Our result is about twice of that ($\sim 5\%$) for $\delta = 0.1$ given in Cao (2007). The discrepancy is mainly attributed to two factors. The first one is that a single average mass accretion rate adopted in Cao (2007) for the calculations of ADAF spectra and their contribution to the XRB, which over-estimated the average radiative efficiency for ADAFs in inactive galaxies, and therefore under-estimate the fraction of local black hole mass accreted during ADAF phases. The another one is that a different AGN population synthesis model for the newly measured XRB with *Swift* is adopted in the calculations in this work. Our present results are roughly consistent with that derived from observed Eddington ratio distributions in Hopkins et al. (2006).

ADAFs are very hot, and the temperature of the ions in ADAFs can be as high as $\sim 10^{12}$K (see Fig. 3), which implies that γ-ray emission may be produced through the pion production processes in the proton-proton (p-p) collisions and subsequently decay of neutral pions (Mahadevan et al. 1997). We calculate their contribution to the extragalactic γ-ray background (EGRB), and find that less than 1% of the observed EGRB is contributed by the ADAFs in these faint sources if the massive black holes are spinning rapidly, while the contribution to the EGRB from ADAFs can be neglected if the black holes are non-rotating (see Figs. 10 and 11). Our results are consistent with the previous works showing that about $\sim 25\%$ to $\sim 100\%$ of the EGRB can be attributed to the unresolved blazars (e.g., Padovani et al. 1993; Chiang et al. 1995; Stecker & Salamon 1996; Mücke & Pohl 2000; Cao & Bai 2008; Bhattacharya et al. 2009).

We thank the anonymous referee for very helpful comments/suggestions, and Treister E. for providing the data of the XRB and their AGN population synthesis model. This work is supported by the NSFC (grants 10778621, 10703003, 10773020, 10821302 and 10833002), the National Basic Research Program of China (grant 2009CB824800), the Science and Technology Commission of Shanghai Municipality (10XD1405000), and the CAS (grant KJCX2-YW-T03).

REFERENCES

Ajello, M., et al. 2008, ApJ, 689, 666
Armitage, P. J. 1998, ApJ, 501, L189
Bhattacharya, D., Sreekumar, P., & Mukherjee, R. 2009, Research in Astronomy and Astrophysics, 9, 1205
Cao, X. 2005, ApJ, 631, L101
Cao, X. 2007, ApJ, 659, 950
Cao, X., & Bai, J. M. 2008, ApJ, 673, L131
Cao, X., & Li, F. 2008, MNRAS, 390, 561
Cao, X., & Xu, Y.-D. 2007, MNRAS, 377, 425
Chiang, J., Fichtel, C. E., von Montigny, C., Nolan, P. L., & Petrosian, V. 1995, ApJ, 452, 156
Churazov, E., et al. 2007, A&A, 467, 529
De Luca, A., & Molendi, S. 2004, A&A, 419, 837
Dermer, C. D. 1986, ApJ, 307, 47
di Matteo, T., & Fabian, A. C. 1997, MNRAS, 286, 393
Elvis, M., Risaliti, G., & Zamorani, G. 2002, ApJ, 565, L75
Ferrarese, L., & Merritt, D. 2000, ApJ, 539, L9
Gebhardt, K., et al. 2000, ApJ, 539, L13
Gilli, R., Comastri, A., & Hasinger, G. 2007, A&A, 463, 79
Giovannelli, F., Karakula, S., & Tkaczyk, W. 1982, A&A, 107, 376
Giovannelli, F., Karakula, S., & Tkaczyk, W. 1982, Acta Astronomica, 32, 121
Hasinger, G. 1998, Astronomische Nachrichten, 319, 37
Hawley, J. F., & Balbus, S. A. 2002, ApJ, 573, 738
Hawley, J.F., Gammie, C.F., & Balbus, S.A. 1996, ApJ, 464, 690
Hickox, R. C., & Markevitch, M. 2006, ApJ, 645, 95
Ho, L. C. 2002, ApJ, 564, 120
Hopkins, P. F., & Hernquist, L. 2009, ApJ, 698, 1550
Hopkins, P. F., Hernquist, L., Cox, T. J., Di Matteo, T., Robertson, B., & Springel, V. 2005, ApJ, 630, 716
Hopkins, P. F., Hernquist, L., Martini, P., Cox, T. J., Robertson, B., Di Matteo, T., & Springel, V. 2005, ApJ, 625, L71
Hopkins, P. F., Narayan, R., & Hernquist, L. 2006, ApJ, 643, 641
Hopkins, P. F., Richards, G. T., & Hernquist, L. 2007, ApJ, 654, 731
Jester, S. 2005, ApJ, 625, 667
Kauffmann, G., & Heckman, T. M. 2009, MNRAS, 397, 135
Kollmeier, J. A., et al. 2006, ApJ, 648, 128
Li, Y.-R., Wang, J.-M., Yuan, Y.-F., Hu, C., & Zhang, S. 2010, ApJ, 710, 878
Mahadevan, R., Narayan, R., & Krolik, J. 1997, ApJ, 486, 268
Manmoto, T. 2000, ApJ, 534, 734
Marconi, A., Risaliti, G., Gilli, R., Hunt, L. K., Maiolino, R., & Salvati, M. 2004, MNRAS, 351, 169
McLure, R. J., & Dunlop, J. S. 2004, MNRAS, 352, 1390
Merloni, A., & Heinz, S. 2008, MNRAS, 388, 1011
Mücke, A., & Pohl, M. 2000, MNRAS, 312, 177
Narayan, R. 2002, Lighthouses of the Universe: The Most Luminous Celestial Objects and Their Use for Cosmology, 405
Narayan, R., Mahadevan, R., & Quataert, E. 1998, in Theory of Black Hole Accretion Disks, edited by Marek A. Abramowicz, Gunnlaugur Bjornsson, and James E. Pringle.
Narayan, R., & Yi, I. 1995, ApJ, 452, 710
Oka, K., & Manmoto, T. 2003, MNRAS, 340, 543
Padovani, P., Ghisellini, G., Fabian, A. C., & Celotti, A. 1993, MNRAS, 260, L21
Salucci, P., Szuszkiewicz, E., Monaco, P., & Danese, L. 1999, MNRAS, 307, 637
Schmidt, M., et al. 1998, A&A, 329, 495
Shankar, F., Salucci, P., Granato, G. L., De Zotti, G., & Danese, L. 2004, MNRAS, 354, 1020
Shankar, F., Weinberg, D. H., & Miralda-Escudé, J. 2009, ApJ, 690, 20
Soltan, A. 1982, MNRAS, 200, 115
Sreekumar, P., et al. 1998, ApJ, 494, 523
Stecker, F. W. 1971, NASA Special Publication, 249
Stecker, F. W., & Salamon, M. H. 1996, ApJ, 464, 600
Treister, E., & Urry, C. M. 2005, ApJ, 630, 115
Treister, E., Urry, C. M., & Virani, S. 2009, ApJ, 696, 110
Ueda, Y., Akiyama, M., Ohta, K., & Miyaji, T. 2003, ApJ, 598, 886
Yu, Q., & Tremaine, S. 2002, MNRAS, 335, 965